



IMPROVING POWER QUALITY OF THE DISTRIBUTION GRID BY USING DYNAMIC VOLTAGE RESTORER ULTRA CAPACITOR

B. DIVYA SREE¹, K. BHASKAR²

¹Working as MATLAB developer and Branch Manager (DSNR) in VISION KREST EMBEDDED TECHNOLOGIES, Private Ltd., Hyderabad

²Working as Senior EMBEDDED developer in VISION KREST EMBEDDED TECHNOLOGIES, Private Ltd., Hyderabad

ABSTRACT: In this paper, UCAP-based energy storage integration to a DVR into the distribution grid is proposed. Dynamic voltage restorer (DVR) is one product that can provide improved voltage sag and swell compensation with energy storage integration. The novel contribution of this paper lies in the integration of rechargeable UCAP-based energy storage into the DVR topology. Here we are using the fuzzy controller compared to other controllers i.e. The fuzzy controller is the most suitable for the human decision-making mechanism, providing the operation of an electronic system with decisions of experts. DVR is the most reliable custom power device that can protect sensitive load and it can be thoroughly solved the power quality problem in distribution power generation. UCAP is integrated into dc-link of the DVR through a bidirectional dc-dc converter, which helps in providing a stiff dc-link voltage, and the integrated UCAP-DVR system helps in compensating temporary voltage sags and voltage swells, which last from 3 s to 1 min. SCAPs are electronic devices which are able of holding huge amount of electrical in trust quantity. By using the fuzzy controller for a nonlinear system allows for a reduction of uncertain effects in the system control and improves the efficiency. It is also called as Ultra Capacitor (UCAP). Complexities involved in the design and control of both the dc-ac inverter and the dc-dc converter are discussed.

Index Terms—DC-DC converter, d-q control, DSP, dynamic voltage restorer (DVR), Fuzzy logic controller, energy storage integration, phase locked loop (PLL), sag/swell, Ultracapacitor (UCAP)

I. INTRODUCTION

Dynamic voltage restorer (DVR) is one product that can provide improved voltage sag and swell compensation with energy storage integration. Ultra capacitors (UCAP) have low-energy density and high-power density ideal characteristics for compensation of voltage sags and voltage swells, which are both events that require high power for short spans of time. In order to avoid and minimize

the active power injection into the grid, the authors also mention an alternative solution which is to compensate for the voltage sag by inserting a lagging voltage in quadrature with the line current. Due to the high cost of rechargeable energy storage, various other types of control strategies have also been developed in the literature [2]–[8] to minimize the active power injection from the DVR. The high cost of the rechargeable energy storage prevents the penetration of the DVR as a power quality product. However, the cost of rechargeable energy storage has been decreasing drastically due to various technological developments and due to higher penetration in the market in the form of auxiliary energy storage for distributed energy resources (DERs) such as wind, solar, hybrid electric vehicles (HEVs), and plug-in hybrid electric vehicle (PHEVs) [9], [10].

Various types of rechargeable energy storage technologies based on superconducting magnets (SMES), flywheels (FESS), batteries (BESS), and ultra capacitors (UCAPs) are compared in [10] for integration into advanced power applications such as DVR. Efforts have been made to integrate energy storage into the DVR system, which will give the system active power capability that makes it independent of the grid during voltage disturbances. To improve the power quality, it is necessary to know what kind of disturbances occurred and quality initially assign to the quality of the service delivered as ‘measured’ by the consumers ability to use the energy delivered in the desire manner.

In this paper, UCAP-based energy storage integration to a DVR into the distribution grid is proposed and the following application areas are addressed. 1) Integration of the UCAP with DVR system gives active power capability to the system, which is necessary for independently compensating voltage sags and swells. 2) Simulation validation of

the UCAP, dc-dc converter, and inverter their interface and control. 3) Development of inverter and dc-dc converter controls to provide sag and swell compensation to the distribution grid.

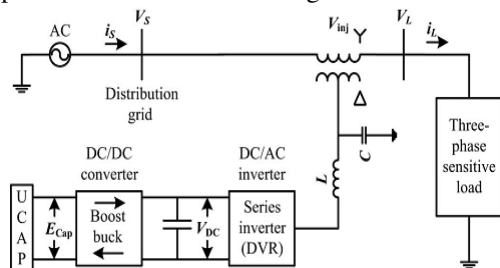


Fig. 1. One-line diagram of DVR with UCAP energy storage

UCAPs have low-energy density and high-power density ideal characteristics for compensating voltage sags and voltage swells, which are both events that require high amount of power for short spans of time. With the prevalence of renewable energy sources on the distribution grid and the corresponding increase in power quality problems, the need for DVRs on the distribution grid is increasing [16].

II. THREE-PHASE SERIES INVERTER

A. Power Stage

The one-line diagram of the system is shown in Fig. 1. The power stage is a three-phase voltage source inverter, which is connected in series to the grid and is responsible for compensating the voltage sags and swells; the model of the series DVR and its controller is shown in Fig. 2.

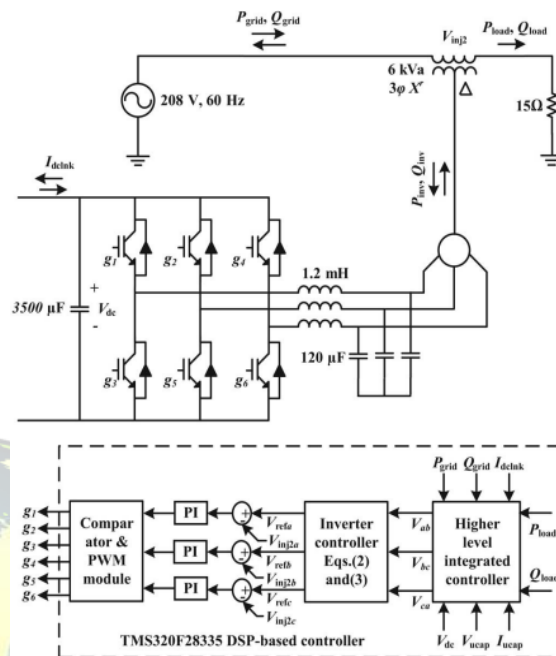


Fig. 2. Model of three-phase series inverter (DVR) and its controller with integrated higher order controller.

The inverter system consists of an insulated gate bipolar transistor (IGBT) module, its gate-driver, LC filter, and an isolation transformer. The dc-link voltage V_{dc} is regulated at 260 V for optimum performance of the converter and the line-line voltage V_{ab} is 208 V; based on these, the modulation index m of the inverter is given by

$$m = \frac{2\sqrt{2}}{\sqrt{3}V_{dc} \cdot n} V_{ab}(rms) \quad (1)$$

Where n is the turns ratio of the isolation transformer. Substituting n as 2.5 in (1), the required modulation index is calculated as 0.52. Therefore, the output of the dc-dc converter should be regulated at 260 V for providing accurate voltage compensation.

B. Controller Implementation

There are various methods to control the series inverter to provide dynamic voltage restoration and most of them rely on injecting a voltage in quadrature with advanced phase, so that reactive power is utilized in voltage restoration. To minimize the active power support and the amount of energy storage requirement at the dc-link is regulated in order to minimize the cost of energy storage. However, the cost of energy storage has been declining and with the availability of active power support at the dc-link, complicated phase-advanced techniques can be avoided and voltages can be

injected in-phase with the system voltage during a voltage sag or a swell event. This requires PLL for estimating θ , which has been implemented using the fictitious power method described in [18]. Based on the estimated θ and the line–line source voltages, V_{ab} , V_{bc} , and V_{ca} (which are available for this delta-sourced system) are transformed into the d–q domain and the line– neutral components of the source voltage V_{sa} , V_{sb} , and V_{sc} , which are not available, can then be estimated using

$$\begin{bmatrix} V_{sa} \\ V_{sb} \\ V_{sc} \end{bmatrix} = \begin{bmatrix} 1 & 0 \\ -1 & \sqrt{3} \\ -1 & -\sqrt{3} \end{bmatrix} \begin{bmatrix} \cos(\theta - \frac{\pi}{6}) & \sin(\theta - \frac{\pi}{6}) \\ -\sin(\theta - \frac{\pi}{6}) & \cos(\theta - \frac{\pi}{6}) \end{bmatrix} \begin{bmatrix} \frac{V_d}{\sqrt{3}} \\ \frac{V_q}{\sqrt{3}} \end{bmatrix} \quad (2)$$

$$\begin{bmatrix} V_{refa} \\ V_{refb} \\ V_{refc} \end{bmatrix} = m * \begin{bmatrix} \sin(\theta - \frac{2\pi}{3}) - \frac{V_{sa}}{169.7} \\ \sin(\theta - \frac{2\pi}{3}) - \frac{V_{sb}}{169.7} \\ \sin(\theta + \frac{2\pi}{3}) - \frac{V_{sc}}{169.7} \end{bmatrix} \quad (3)$$

$$\begin{aligned} P_{inv} &= 3V_{inj2a(rms)}I_{La(rms)}\cos\phi \\ Q_{inv} &= 3V_{inj2a(rms)}I_{La(rms)}\sin\phi \end{aligned} \quad (4)$$

These voltages are normalized to unit sine waves using line– neutral system voltage of 120 Vrms as reference. Therefore, whenever there is a voltage sag or swell on the source side, a corresponding voltage V_{inj2} is injected in-phase by the DVR and UCAP system to negate the effect and retain a constant voltage V_L at the load end. The actual active and reactive power supplied by the series inverter can be computed using (4) from the rms values of the injected voltage V_{inj2a} and load current I_{La} , and ϕ is the phase difference between the two waveforms.

III. UCAP AND BIDIRECTIONAL DC–DC CONVERTER

A. UCAP Bank Hardware Setup

The choice of the number of UCAPs necessary for providing grid support depends on the amount of support needed, terminal voltage of the UCAP, dc-link voltage, and distribution grid voltages. It is practical and cost-effective to use three modules in the UCAP bank. Assuming that the UCAP bank can be discharged to 50% of its initial voltage ($V_{uc,ini}$) to final voltage ($V_{uc,fin}$) from 144 to 72 V, which translates to depth of discharge of

75%, the energy in the UCAP bank available for discharge is given by

$$\begin{aligned} E_{UCAP} &= \frac{1}{2} * C * \frac{(V_{uc,ini}^2 - V_{uc,fin}^2)}{60} W - min \\ E_{UCAP} &= \frac{1}{2} * 165/3 * (144^2 - 72^2)/60 \\ &= 7128 W-min \end{aligned} \quad (5)$$

B. Bidirectional DC–DC Converter and Controller

A UCAP cannot be directly connected to the dc-link of the inverter like a battery, as the voltage profile of the UCAP varies as it discharges energy. Therefore, there is a need to integrate the UCAP system through a bidirectional dc–dc converter, which maintains a stiff dc-link voltage, as the UCAP voltage decreases while discharging and increases while charging.

The model of the bidirectional dc–dc converter and its controller are shown in Fig. 3

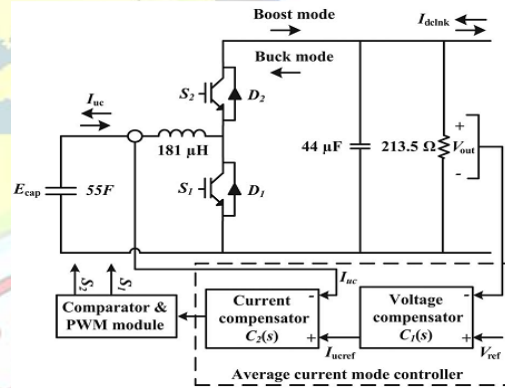


Fig. 3. Model of the bidirectional dc–dc converter and its controller.

The amount of active power support required by the grid during a voltage sag event is dependent on the depth and duration of the voltage sag, and the dc–dc converter should be able to withstand this power during the discharge mode.

The dc–dc converter should also be able to operate in bidirectional mode to be able to charge or absorb additional power from the grid during voltage swell event. In this paper, the bidirectional dc–dc converter acts as a boost converter while discharging power from the UCAP and acts as a buck converter while charging the UCAP from the grid. This method tends to be more stable when compared to other methods such as voltage mode control and peak current mode control. [3] discussed about Improved Particle Swarm Optimization. The fuzzy filter based on particle swarm optimization is used to remove the high density image impulse noise, which occur

during the transmission, data acquisition and processing. The proposed system has a fuzzy filter which has the parallel fuzzy inference mechanism, fuzzy mean process, and a fuzzy composition process. In particular, by using no-reference Q metric, the particle swarm optimization learning is sufficient to optimize the parameter necessitated by the particle swarm optimization based fuzzy filter, therefore the proposed fuzzy filter can cope with particle situation where the assumption of existence of “ground-truth” reference does not hold. The merging of the particle swarm optimization with the fuzzy filter helps to build an auto tuning mechanism for the fuzzy filter without any prior knowledge regarding the noise and the true image. Thus the reference measures are not need for removing the noise and in restoring the image. The final output image (Restored image) confirm that the fuzzy filter based on particle swarm optimization attain the excellent quality of restored images in term of peak signal-to-noise ratio, mean absolute error and mean square error even when the noise rate is above 0.5 and without having any reference measures.

Average current mode controller is shown in Fig. 3, where the dc-link and actual output voltage V_{out} is compared with the reference voltage V_{ref} and the error is passed through the voltage compensator $C1(s)$, which generates the average reference current I_{uref} . When the inverter is discharging power into the grid during voltage sag event, the dc-link voltage V_{out} tends to go below the reference V_{ref} and the error is positive; I_{uref} is positive and the dc-dc converter operates in boost mode. When the inverter is absorbing power from the grid during voltage swell event or charging the UCAP, V_{out} tends to increase above the reference V_{ref} and the error is negative; I_{uref} is negative and the dc-dc converter operates in buck mode. Therefore, the sign of the error between V_{out} and V_{ref} determines the sign of I_{uref} and thereby the direction of operation of the bidirectional dc-dc converter. The reference current I_{uref} is then compared to the actual UCAP current (which is also the inductor current) I_{uc} and the error is then passed through the current compensator $C2(s)$. The compensator transfer functions, which provide a stable response, are given by

$$C_1(S) = 1.67 + \frac{23.81}{s} \quad (6)$$

$$C_2(S) = 3.15 + \frac{1000}{s} \quad (7)$$

IV. FUZZY LOGIC CONTROLLER

In FLC, basic control action is determined by a set of linguistic rules. These rules are determined by the system. Since the numerical variables are converted into linguistic variables, mathematical modeling of the system is not required in FC. The FLC comprises of three parts: fuzzification, inference engine and defuzzification. The FC is characterized as i. seven fuzzy sets for each input and output. ii. Triangular membership functions for simplicity. iii. Fuzzification using continuous universe of discourse. iv. Implication using Mamdani's, 'min' operator. v. Defuzzification using the height method.

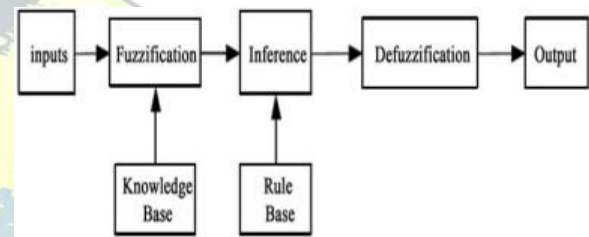


Fig.4.Fuzzy logic controller

TABLE I: Fuzzy Rules

e \dot{e}	NB	NM	NS	ZE	PS	PM	PB
NB	NB	NB	NB	NB	NM	NS	ZE
NM	NB	NB	NB	NM	NS	ZE	PS
NS	NB	NB	NM	NS	ZE	PS	PM
ZE	NB	NM	NS	ZE	PS	PM	PB
PS	NM	NS	ZE	PS	PM	PB	PB
PM	NS	ZE	PS	PM	PB	PB	PB
PB	ZE	PS	PM	PB	PB	PB	PB

Fuzzification: Membership function values are assigned to the linguistic variables, using seven fuzzy subsets: NB (Negative Big), NM (Negative Medium), NS (Negative Small), ZE (Zero), PS (Positive Small), PM (Positive Medium), and PB (Positive Big). The Partition of fuzzy subsets and the shape of membership $\mu_{E(k)}$ function adapt the shape up to appropriate system. The value of input error and change in error are normalized by an input scaling factor. In this system the input scaling factor has been designed such that input values are between -1 and +1. The triangular shape of the membership function of this arrangement presumes that for any particular

$E(k)$ input there is only one dominant fuzzy subset. The input error for the FLC is given as

$$E(k) = \frac{P_{ph(k)} - P_{ph(k-1)}}{V_{ph(k)} - V_{ph(k-1)}} \quad (8)$$

$$CE(k) = E(k) - E(k-1) \quad (9)$$

Inference Method: Several composition methods such as Max-Min and Max-Dot have been proposed in the literature. In this paper Min method is used. The output membership function of each rule is given by the minimum operator and maximum operator. Table 1 shows rule base of the FLC.

Defuzzification: As a plant usually requires a non-fuzzy value of control, a defuzzification stage is needed. To compute the output of the FLC, „height“ method is used and the FLC output modifies the control output. Further, the output of FLC controls the switch in the inverter. In UPQC, the active power, reactive power, terminal voltage of the line and capacitor voltage are required to be maintained. In order to control these parameters, they are sensed and compared with the reference values. To achieve this, the membership functions of FC are: error, change in error and output

The set of FC rules are derived from

$$u = -[\alpha E + (1-\alpha)C] \quad (10)$$

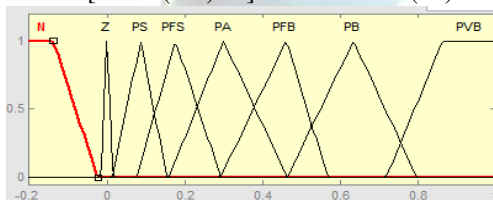


Fig.5 input error as membership functions

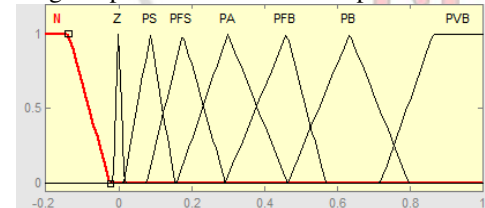


Fig.6 change as error membership functions

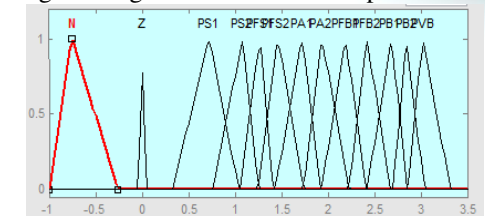


Fig.7 output variable Membership functions

Where α is self-adjustable factor which can regulate the whole operation. E is the error of the system, C is the change in error and u is the control variable.

V. SIMULATION RESULTS

The simulation of the proposed UCAP-integrated DVR system is carried out in PSCAD for a 208 V, 60-Hz system where 208 V is 1 p.u. The system response for a three-phase voltage sag, which lasts for 0.1 s and has a depth of 0.84 p.u., is shown in Fig. 8(a)–(e).

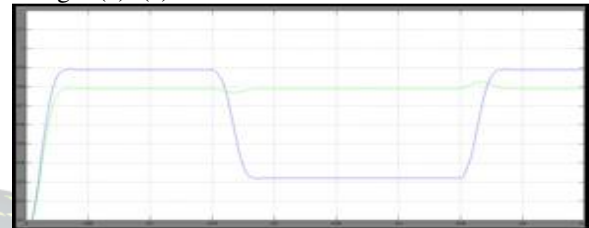


Fig. 8 (a): Source and load RMS voltages V_{rms} and VL_{rms} during sag.

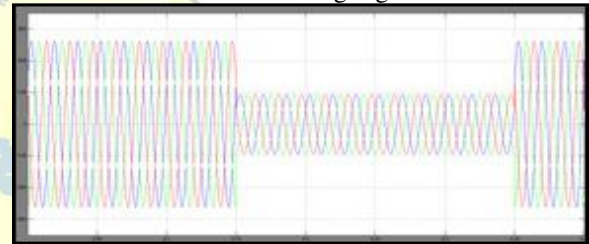


Fig 8(b): Source voltages V_{sab} (blue), V_{sbc} (red), and V_{sca} (green) during sag.

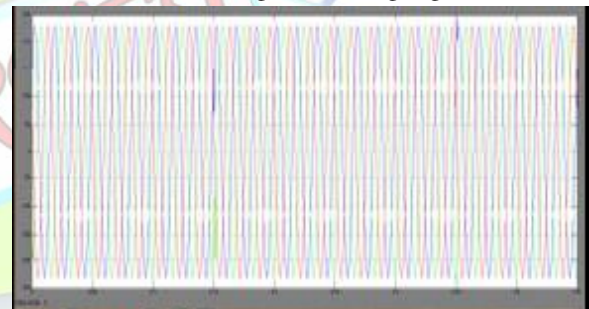


Fig 8(c): Load voltages V_{Lab} (blue), V_{Lbc} (red), and V_{Lca} (green) during sag

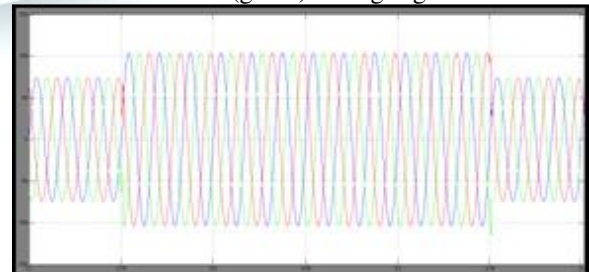


Fig 8 (d): Injected voltages V_{inj2a} (blue), V_{inj2b} (red), and V_{inj2c} (green) during sag.

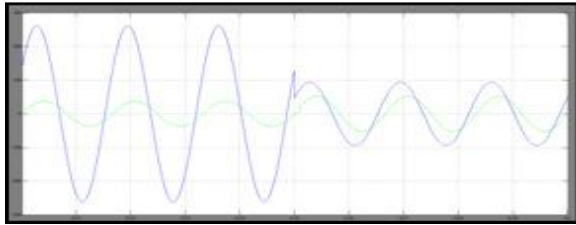
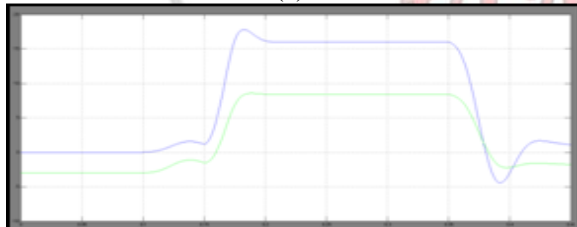


Fig 8(e): Vinj2a (green) and Vsab (blue) waveforms during sag

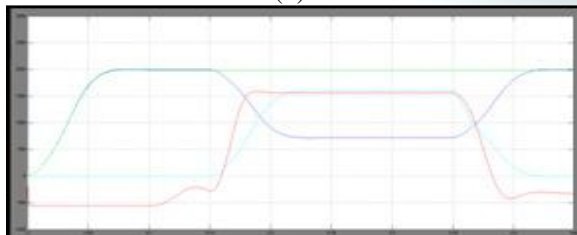
In Fig. 9(a), plots of the bidirectional dc-dc converter are presented and it can be observed that the dc-link voltage V_{dc} is regulated at 260 V, the average dc-link current I_{dc} and the average UCAP current I_{ucav} increase to provide the active power required by the load during the sag. Although the UCAP is discharging, the change in the UCAP voltage E_{cap} is not visible in this case due to the short duration of the simulation, which is due to limitations in PSCAD software. It can also be observed from the various active power plots shown in Fig. 9(b) where the power supplied to the load P_{load} remains constant even during the voltage sag when the grid power P_{grid} is decreasing.



(a)



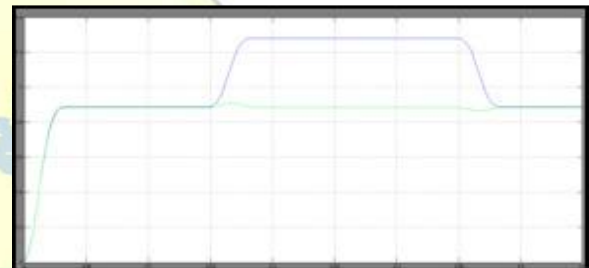
(b)



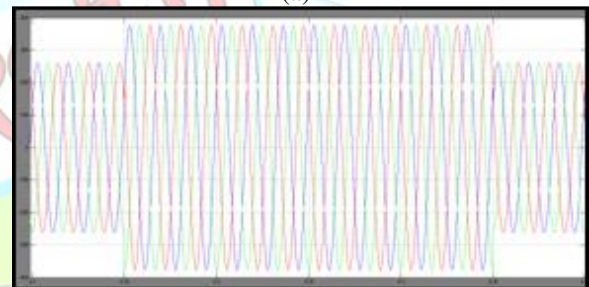
(c)

Fig. 9: (a) Currents and voltages of dc-dc converter. (b) Active power of grid, load, and inverter during voltage sag.

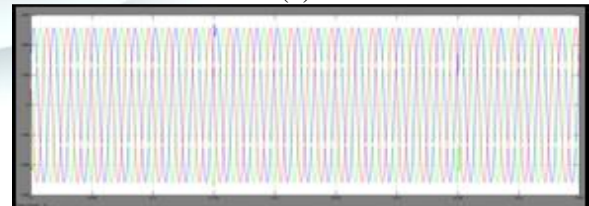
The active power requirement is greatest for the case where all the three phases ABC experience voltage sag. The system response for a three-phase voltage swell, which lasts for 0.1 s and has a magnitude of 1.2p.u., is shown in Fig. 10(a)–(e). It can be observed that during voltage swell, the source voltage V_{rms} increases to 1.2p.u., whereas the load voltage V_{Lrms} is maintained constant at around 1p.u. due to voltages injected in-phase by the series inverter. It can be observed from the inverter power P_{inv} and inverter input power P_{dc} in plots that the additional active power from the grid is absorbed by the inverter and transmitted to the UCAP. Therefore, it can be concluded from the plots that the additional active power from the grid during the voltage swell event is being absorbed by the UCAP-DVR system through the bidirectional dc-dc converter and the inverter.



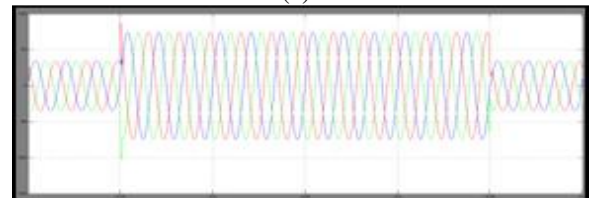
(a)



(b)



(c)



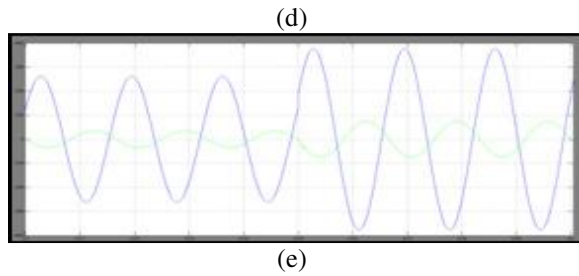


Fig.10: (a) Source and load rms voltages V_{srms} and V_{Lrms} during swell. (b) Source voltages V_{sab} (blue), V_{sbc} (red), and V_{sca} (green) during swell. (c) Load voltages V_{Lab} (blue), V_{Lbc} (red), and V_{Lca} (green) during swell. (d) Injected voltages V_{inj2a} (blue), V_{inj2b} (red), V_{inj2c} (green) during swell. (e) V_{inj2a} (green) and V_{sab} (blue) waveforms during swell.

In Fig. 11(a) and (b), the simulation waveforms of the inverter and the bidirectional dc-dc converter are shown for the case where the grid experiences voltage sag of 0.84 p.u. magnitude for 1-min duration.

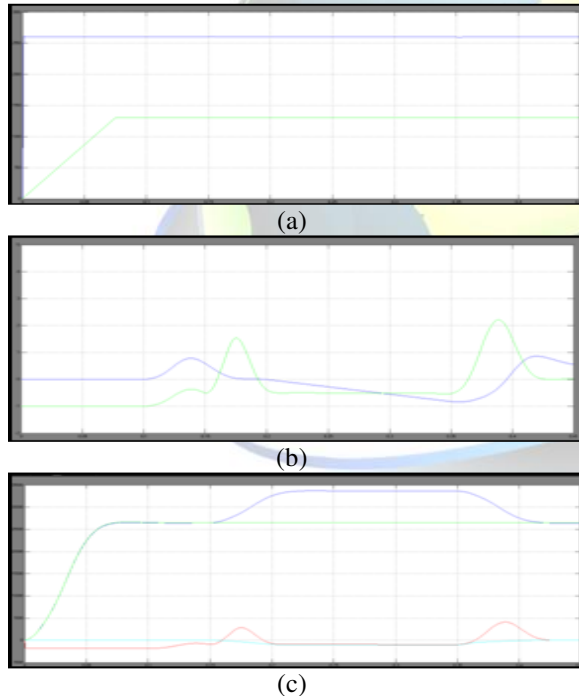


Fig.11: (a) Currents and voltages of dc-dc converter during swell. (b) Active and reactive power of grid, load, and inverter during a voltage swell. Table I, the inverter and the bidirectional dc-dc converter experimental results are presented for both the sag and swell cases.

TABLE I
SERIESINVERTER ANDDC-DC
CONVERTEREXPERIMENTALRESULTS

Series inverter experimental results						
Zone	ϕ	V_{inj2a} (V)	I_{La} (A)	P_{inv} (W)	P_{dc} (W)	η (%)
Sag	0°	102.5	6.8	2091	2206	94.7
Swell	225°	42.43	6.7	-603	-494	83.3
DC-DC converter experimental results						
Zone	E_{cap} (V)	I_{ucav} (A)	I_{dcink} (A)	P_{in} (W)	P_{out} (W)	η (%)
Sag	126.0	19.0	8.1	2406.6	2206	91.6
Swell	106.0	-4.0	1.9	-494.0	-424.0	85.8

VI. CONCLUSION

The UCAP integration through a bidirectional dc-dc converter at the dc-link of the DVR is proposed. In this paper, the concept of integrating UCAP-based rechargeable energy storage to the DVR system to improve its voltage restoration capabilities is explored. Dynamic voltage restoration is a process and instrument necessity to maintain, or restore and also compensate functional electric load during voltage sag and swell, harmonics in voltage supply. DVR is the most reliable custom power device that can protect sensitive load and it can be thoroughly solved the power quality problem in distribution power generation. With this integration, the DVR will be able to independently compensate voltage sags and swells without relying on the grid to compensate for faults on the grid. The integration of this technology into the distribution power generation, power quality is being enhanced since these devices gives quick response and high reliability. The control strategy is simple and is based on injecting voltages in-phase with the system voltage and is easier to implement when the DVR system has the ability to provide active power. UCAP based energy storages can be deployed in the future on the distribution grid to respond to dynamic changes in the voltage profiles of the grid and prevent sensitive loads from voltage disturbances.

REFERENCES

- [1] N. H. Woodley, L. Morgan, and A. Sundaram, "Experience with an inverter-based dynamic voltage restorer," IEEE Trans. Power Del., vol. 14, no. 3, pp. 1181-1186, Jul. 1999.
- [2] S. S. Choi, B. H. Li, and D. M. Vilathgamuwa, "Dynamic voltage restoration with minimum energy injection," IEEE Trans. Power Syst., vol. 15, no. 1, pp. 51-57, Feb. 2000.
- [3] Christo Ananth, Vivek.T, Selvakumar.S., Sakthi Kannan.S., Sankara Narayanan.D, "Impulse Noise Removal using Improved Particle Swarm



Optimization", International Journal of Advanced Research in Electronics and Communication Engineering (IJARECE), Volume 3, Issue 4, April 2014, pp 366-370

[4] Y. W. Li, D. M. Vilathgamuwa, F. Blaabjerg, and P. C. Loh "A robust control scheme for medium-voltage-level DVR implementation," IEEE Trans. Ind. Electron., vol. 54, no. 4, pp. 2249–2261, Aug. 2007.

[5] A. Ghosh and G. Ledwich, "Compensation of distribution system voltage using DVR," IEEE Trans. Power Del., vol. 17, no. 4, pp. 1030–1036, Oct. 2002.

[6] A. Elnady and M. M. A. Salama, "Mitigation of voltage disturbances using adaptive perceptron-based control algorithm," IEEE Trans. Power Del., vol. 20, no. 1, pp. 309–318, Jan. 2005.

[7] P. R. Sanchez, E. Acha, J. E. O. Calderon, V. Feliu, and A. G. Cerrada, "A versatile control scheme for a dynamic voltage restorer for power quality improvement," IEEE Trans. Power Del., vol. 24, no. 1, pp. 277–284, Jan. 2009.

[8] C. S. Lam, M. C. Wong, and Y. D. Han, "Voltage swell and overvoltage compensation with unidirectional power flow controlled dynamic voltage restorer," IEEE Trans. Power Del., vol. 23, no. 4, pp. 2513–2521, Oct. 2008.

[9] K. Sahay and B. Dwivedi, "Supercapacitor energy storage system for power quality improvement: An overview," J. Elect. Syst., vol. 10, no. 10, pp. 1–8, 2009.

[10] P. F. Ribeiro, B. K. Johnson, M. L. Crow, A. Arsoy, and Y. Liu, "Energy storage systems for advanced power applications," Proc. IEEE, vol. 89, no. 12, pp. 1744–1756, Dec. 2001.

[11] H. K. Al-Hadidi, A. M. Gole, and D. A. Jacobson, "A novel configuration for a cascaded inverter-based dynamic voltage restorer with reduced energy storage requirements," IEEE Trans. Power Del., vol. 23, no. 2, pp. 881–888, Apr. 2008.

[12] R. S. Weissbach, G. G. Karady, and R. G. Farmer, "Dynamic voltage compensation on distribution feeders using flywheel energy storage," IEEE Trans. Power Del., vol. 14, no. 2, pp. 465–471, Apr. 1999.

[13] A. B. Arsoy, Y. Liu, P. F. Ribeiro, and F. Wang, "StatCom-SMES," IEEE Ind. Appl. Mag., vol. 9, no. 2, pp. 21–28, Mar. 2003.

[14] C. Abbey and G. Joos, "Supercapacitor energy storage for wind applications," IEEE Trans. Ind. Appl., vol. 43, no. 3, pp. 769–776, Jun. 2007.

[15] S. Santoso, M. F. McGranaghan, R. C. Dugan, and H. W. Beaty, Electrical Power Systems Quality,

3rd ed. New York, NY, USA: McGraw-Hill, Jan. 2012.

AUTHORS PROFILE:



B. Divya Sree is currently working as MATLAB developer and Branch Manager (DSNR) in VISION KREST EMBEDDED TECHNOLOGIES, Private Ltd., Hyderabad. She received her Master of Technology degree in ELECTRICAL POWER ENGINEERING from CVR College of Engineering, Ibrahimpatnam, Hyderabad, Telangana; she received her Bachelor of Engineering degree from Vijay College of Engineering for women, Nizamabad. Her areas of interest are Electrical Power Systems and FACTS.

Email id: divyasrees.balipogula@gmail.com



Mr. K. Bhaskar is currently working as Senior EMBEDDED developer in VISION KREST EMBEDDED TECHNOLOGIES, Private Ltd., Hyderabad. He completed his M.Tech in Embedded Systems and completed his B.Tech in Electrical and Electronics Engineering from Joginipally B. R. Engineering College, Hyderabad and also completed his Diploma in Electrical and Electronics Engineering from Govt. Polytechnic College, Warangal. His Interested areas of Research include Embedded Systems, R&D Department, Electrical MATLAB Designing, Internet of Things, Digital Electronics and Hardware Design.